Surface/interface electronic structure in C 60 anchored aminothiolate self-assembled monolayer: An approach to molecular electronics

Archita Patnaik, Hiroyuki Setoyama, and Nobuo Ueno

Citation: The Journal of Chemical Physics **120**, 6214 (2004); doi: 10.1063/1.1651062
View online: http://dx.doi.org/10.1063/1.1651062
View Table of Contents: http://scitation.aip.org/content/aip/journal/jcp/120/13?ver=pdfcov
Published by the AIP Publishing

Surface/interface electronic structure in C_{60} anchored aminothiolate self-assembled monolayer: An approach to molecular electronics

Archita Patnaik[a)]
Department of Chemistry, Indian Institute of Technology Madras, Chennai 600036, India

Hiroyuki Setoyama and Nobuo Ueno
Department of Materials Technology, Chiba University, Yayoi-cho, Inageku, Chiba 2638522, Japan

(Received 20 October 2003; accepted 6 January 2004)

Electronic structure in self-assembled monolayers (SAMs) of C_{60} anchored 11-amino–1-undecane thiol (C_{60}-11-AUT) on Au(111) was studied by means of ultraviolet photoelectron spectroscopy and hybrid density functional theory calculations. Valence band features of the molecular conformation revealed the interface electronic structure to be dominated by σ(S–Au), localized at the thiolate anchor to Au. Formation of a localized covalent bond as a result of hybridization between N P_z orbital of $-NH_2$ group of the thiolate SAM and the π level of C_{60} resulted in a symmetry change from I_h in C_{60} to C1 in C_{60}-11-AUT SAM. Appearance of low, but finite amplitude surface electronic states of bonded C_{60}, much beyond the Fermi level, ruled out Au–C_{60} end group contact. The band gap E_g of the SAM, determined to be 2.7 eV, was drastically reduced from the insulating alkanethiol SAMs (~8.0 eV) and fell intermediate between the C_{60} ground state (N electrons, 1.6 eV) and C_{60} solid (N±1 electrons, 3.7 eV). © *2004 American Institute of Physics.*
[DOI: 10.1063/1.1651062]

I. INTRODUCTION

The quantum mechanical nature of electron conduction along with the several possibilities for structural modification in organic molecules and their self-assembly are critical for fabrication of nanometer-scale electronic devices. Recent developments in the concept of molecular electronics as ''single molecule'' conduction was put forward by Reed *et al.*,[1] where molecules of benzene-1,4-dithiol self assembled onto the two facing gold electrodes allowed direct observation of charge transport. Following this, 2′-amino-4-ethynylphenyl-4′-ethynylphenyl-5′-nitro-1-benzenethiol), containing a nitroamine redox center was reported as a potential molecular quantum wire.[2] While the interfacial electronic structure/electronic coupling between molecular orbitals and the metal substrate has been undertaken sufficiently theoretically,[3–7] the corresponding experimental reports probing the surface/interface electronic structure is scarce. The work of Emberly and Kirczenow[6] showed that the surface bonding can be strong enough to distort the electronic structure of the molecule. Using laser two-photon photoemission spectroscopy, recent experiments, in conjunction with electronic structural calculations on self-assembled monolayers (SAMs) of pentafluorothiophenolate ($C_6F_5S^-$) on Cu(111),[8] probed the interface electronic structure. Strong electronic coupling/direct wave function mixing between the metal and the molecular orbitals via the S bridge was attributed to stabilization of the molecular state. In subsequent experiments,[9] these authors found that the electronic structure in thiophenolate SAM as well as in octylthiolate and ethylthiolate SAMs is dominated by two virtual orbitals, localized to the thiolate anchor and strongly coupled to the metal substrate. The shapes and energies of interfacial σ^*-like orbitals were found independent of the nature of hydrocarbon group, irrespective of saturated alkyls or conjugated aromatics. Direct observation of S–Au bonding state in 8-bromo-1-octanethiol SAM on Au(111) from ethanol solution was reported by Kera *et al.*[10] Thus, studying SAMs with redox-active groups in context to understanding their surface/interface properties/electronic structure plays a fundamental importance in molecular technology.

The unique electronic, spectroscopic, and structural properties of fullerenes and fullerene based material thin films warrant successful technological application of these thin films, which relies on their rational chemical modification, and development of methodologies to arrange them on variety of highly ordered molecular surfaces. In order to obtain well-defined two-dimensional fullerene structure, C_{60} SAMs have been prepared by using various linkages such as amine,[11–13] azide,[14] and pyrrolidine ring,[15] where the π delocalization of C_{60} is disrupted by these surface tailoring groups upon formation of σ bonds. However, these molecular adhesion agents or glues have become increasingly important in the construction of new materials, specifically used for surface immobilization of nanostructures. The amine and amide terminated SAMs as molecular glues for Au(111) and SiO_2 substrates have shown ~70% of the amine groups in $-NH_2$ chemical state after the process of self assembly.[16] An appropriate selection of the end group of a SAM assembly, such as C_{60} as an electron acceptor, would render the resultant SAM on the Au surface a potential system for studying fundamentals of electron transfer processes at the interfaces. In this work, we investigated the surface/interface electronic

a)Author to whom correspondence should be addressed. Present address: JSPS Invitation Fellow, Chiba University, Japan; Electronic mail: archita59@yahoo.com

structure of C_{60}-11-amino–1-undecane thiol (AUT) SAM using ultraviolet photoelectron spectroscopy (UPS) that probes both the occupied states. Upon binding C_{60} to an amine-terminated alkanethiol SAM, we found the interface to be a σ(S–Au) feature highest occupied molecular orbital (HOMO), whereas the lowest unoccupied molecular orbital (LUMO), LUMO+1 and LUMO+2 arose from typical C_{60} wave functions. From the measured ionization potentials from valence band photoemission experiments and the C $1s$ core level shakeup feature from x-ray photoelectron spectroscopy (XPS), the HOMO–LUMO electron energy band gap, E_g, was estimated to be 2.7 eV. In the absence of literature on the Fermi level alignment in metal–SAM systems and the electronic band gaps, this study provides a new finding.

II. EXPERIMENT

Controlling nanoscale surface properties vastly depends on the abundance, type, and spatial distribution of tail group sites. We have targeted the covalent attachment of C_{60} to well-defined SAMs of 11-amino-1-undecane thiol [11-AUT] on Au(111) as a matrix to support the C_{60} terminated 11-AUT monolayers. The fullerenes were chosen to be connected to the organosulphur moiety via the amino group, which is small and can thus circumvent steric effects near the bonded C_{60}. Further, the chemistry of functionalizing C_{60} with $-NH_2$ group[17] is a well-established nucleophilic addition reaction at one of the 6:6 double bonds of the carbon cage.

A. Materials

11-amino-1-undecane thiol hydrochloride [HS–$(CH_2)_{11}$–$NH_3^+Cl^-$] was purchased from Dojindo laboratories, Co. Japan. C_{60} of 99.95% purity was used without any further purification. Ethanol (AR grade) and toluene (AR grade) were purchased from Aldrich Chemicals Co. and used as received.

B. Vacuum deposition of Au(111) on mica and preparation of C_{60} film

For this purpose, freshly cleaved 4×4 cm^2 mica strips were preheated by resistive heating at 300 °C for 8 h in order to enhance formation of large Au(111) terraces. Keeping the mica substrate's temperature at ~150 °C, gold evaporation was carried out at 10^{-8} Torr pressure and with a deposition rate of ~0.3 nm/s. Thickness of the Au layer was estimated to be ~100 nm. X-ray diffraction analysis indicated oriented Au(111) polycrystal formation. On the Au films thus formed, C_{60}(99.5%) deposition was carried out at 10^{-8} Torr in a Knudsen cell operating at 603 K. The thickness of the film measured with a quartz crystal monitor was ~140 nm.

C. Monolayer preparation

Self-assembled monolayers of 11-AUT were prepared by immediately soaking the annealed (200 °C for 3 h) gold coated mica strips in ~1 mM 11-AUT ethanol solution at room temperature for 24 h. The aminothiolate SAMs thus formed were exhaustively cleaned with ethanol to get rid of the physisorbed moieties and were immediately dipped further in a freshly prepared ~1 mM C_{60} solution in benzene and kept for 24 h. The SAMs thus formed were washed with benzene, ethanol, and dichloromethane and used for respective experimental investigations after drying in air. The absence of characteristic NH_3^+ vibrations in the Fourier transform infrared spectrum at 3100 cm^{-1} indicated the terminal group of the SAM to be in its free $-NH_2$ state and not in the protonated form.[18]

D. Photoelectron spectroscopy experiments

The UPS spectra were acquired using He I radiation ($h\nu=21.22$ eV). Photoelectron spectra were recorded under an instrumental resolution of 0.22 eV as determined from the Fermi edge measurements of gold. An energy scanning step of 0.05 eV was used. Incidence angle of the photons was 30° with respect to the surface normal and the spectra were recorded at 60°. The vacuum levels of the samples were determined by linear extrapolation of the onset of secondary electrons on the low kinetic energy side of the UPS spectra, which were measured with samples biased at −5 V in order to avoid the influence of the detector work function.

XPS measurements were carried out on a VG CLAM IV spectrometer equipped with a monochromatic Mg $K\alpha$ x-ray source ($h\nu=1253.6$ eV) and at 10^{-10} Torr. The takeoff angle and angle of incidence from the surface normal was employed as 45° for each sample. The sample chamber had a five-axis sample manipulator, *X*, *Y*, *Z*, rotate, and tilt. High-resolution spectra were recorded from the 1×1 mm spot size and were referenced to Au $4f_{7/2}$ at 83.7 eV.

III. RESULTS AND DISCUSSION

A. Computation of the model molecule

To interpret the HOMO and the near HOMO regions in the experimental UPS, hybrid density functional theory (DFT) treatment was carried out on C_{60}-11-AUT with the S atom adsorbed at the threefold hollow site of the Au hexagonal lattice, leading to a $\sqrt{3}\times\sqrt{3}R$ 30° overlayer structure. Calculations were done using the G98W package[19] employing the Becke's three parameter exchange functional[20] combined with the Lee, Yang, and Parr's correlation functional (B3LYP),[21] as implemented in the G98W package. Molecular geometry optimization was done at the B3LYP level of electronic structure theory using LANL2DZ basis set that provides effective core potentials of the double-zeta type.[22] Single point unconstrained calculations were done for obtaining the electronic states. The present B3LYP/LANL2DZ computed structure of the model compound [3 Au–S–$(CH_2)_{11}$–NH_2–C_{60}], shown in Fig. 1, depicts three Au atoms occupying the vertexes of an equilateral triangle with a side length of 2.54 Å. The sulphur atom is seen equidistant from the three Au atoms at 2.28 Å. The C–S distance is found to be 1.83 Å along with Au–S–C bond angle as 114.37°. *Ab initio* geometry optimization of thiol on Au and Ag has shown a preferred geometry for this surface[23,24] along with good experimental evidence.[25] The

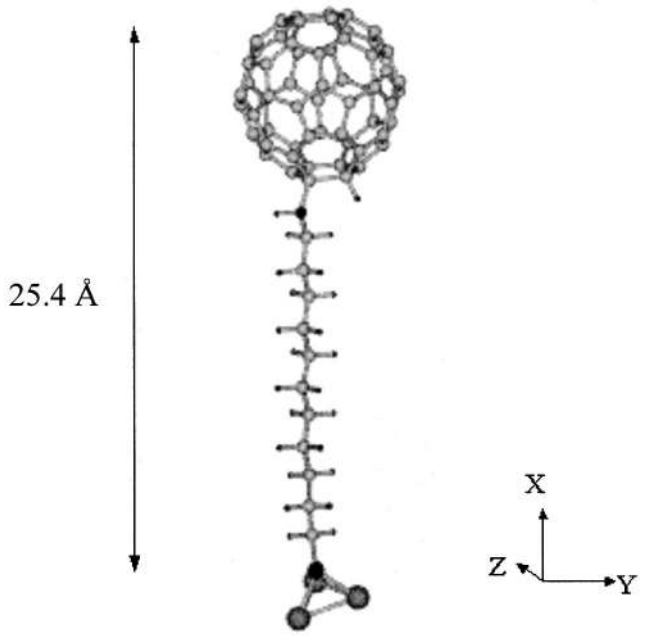

FIG. 1. The molecular conformation and the energy minimized structure of C_{60}-11-AUT SAM from DFT calculations with B3LYP correlation and basis set LANL2DZ. The estimated length of the molecule is shown with S atom bonded to the threefold hollow site of gold hexagonal lattice, forming an arrangement of $(\sqrt{3}\times\sqrt{3})R30°$ overlayer structure. Au and H atoms are shown in deep gray, N and S in black, and C atoms in light gray.

strength of DFT as a first principles tool has been justified with molecule/Au–electrode contacts[26] and with self-assembled monolayers.[8,9]

B. UPS of C_{60}-11-AUT SAM

Figure 2(a) shows the He I (21.22 eV) UPS of the C_{60}-11-AUT SAM on the Au(111) substrate. The formation of the monolayer decreases the work function from 4.5 eV in clean Au(111) to 4.1 eV in the SAM, implying an increase in the secondary electron yield from the adsorbed monolayer on the surface. Yoshimura *et al.*[27] reported gold work function of 4.78 eV in compliance with the present work; work function for alkylthiolate SAMs on Cu(111)[15] decreased to 3.7 eV from 4.9 eV on Cu(111). The photoemission characteristics of the $-NH_2$ terminated thiolate (11-AUT) SAM is shown in the inset. A low but distinct intensity in the HOMO region, when expanded and deconvoluted (spectrum not shown), yielded the HOMO [σ(S–Au)] at 5.9 eV; accordingly, the simulated spectrum [the calculated density of states (DOS)] was shifted by 1.7 eV to fit the experimental spectrum with respect to the HOMO. The nonbonding nitrogen feature is thus observed at 7.8 eV in the inset. The magnitude of this shift is almost similar to a typical value of polarization energy. In the absence of gas phase data for the aminothiol, a comparison with the reported ionization energy, 9.44 eV for *n*-propylamine, yielded a difference of 1.6 eV from the observed value of 7.8 eV.[28] Relaxation energy on the order of 1.7 eV has been reported for SAMs of thiophenol on Au(111).[29]

The spectrum in Fig. 2(a) is accompanied by low intensity in the HOMO and near HOMO regions. The first deriva-

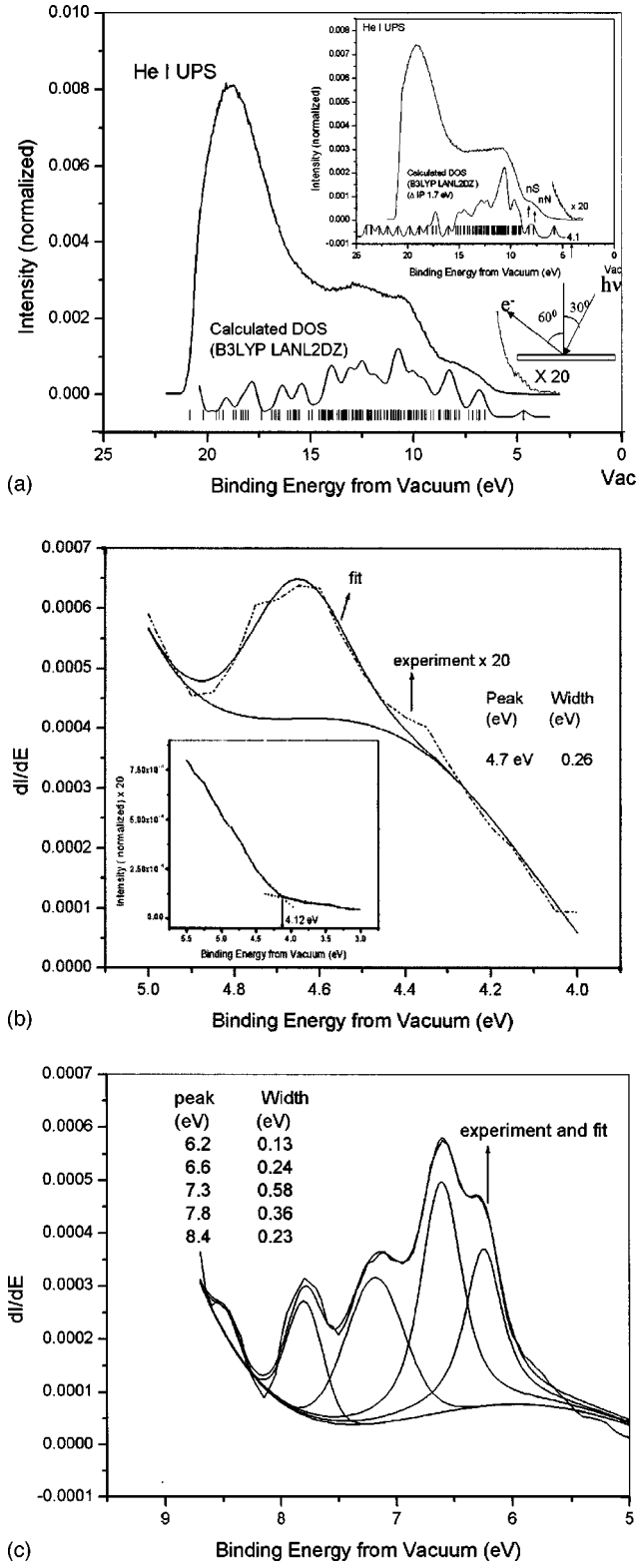

FIG. 2. (a) He I UPS of C_{60}-11-AUT SAM on Au(111) substrate. The calculated DOS of the model molecule (in Fig. 1) is shown with vertical bars representing MO energies obtained from DFT method (B3LYP/LANL2DZ). The DOS curve was calculated by the Gaussian broadening of the energy levels with a width of 0.5 eV. The inset shows He I UPS of 11-AUT SAM showing the position of nonbonding Nitrogen (nN) orbital at 7.8 eV. (b) The first derivative plot of the HOMO in the UPS of C_{60}-11-AUT SAM. (Inset) HOS, the HOMO cutoff at 4.12 eV. (c) The deconvoluted first derivative plot of the near HOMO region in the UPS of C_{60}-11-AUT SAM showing the valence band features.

tive plot in Fig. 2(b) and the deconvoluted first derivative plot in Fig. 2(c) show a distinct broad HOMO in the UPS and emergence of new states above it, respectively. In the inset of Fig. 2(b), the highest occupied state (HOS)/HOMO cutoff of the adsorbed C_{60}-11-AUT SAM is observed at 4.1 eV from the vacuum level, with the HOMO peak maximum at 4.67 eV. In order to characterize the experimental features in Figs. 2(b) and 2(c), the simulated spectrum shown in Fig. 2(a) was derived from the DOS of the model molecule $3\,Au{-}S{-}(CH_2)_{11}{-}NH_2{-}C_{60}$, calculated from DFT with B3LYP correlation. The process convoluted the delta functions at the energies of occupied states with a Gaussian function of 0.5 eV full width at half maximum. The longitudinal bars represent calculated binding energy of each state. The energy scale of the simulated spectrum was shifted 0.5 eV to the higher binding energy side to coincide with the experimental HOMO energy.

C. The σ(S–Au) interface

In Figs. 3(a), 3(b), and 3(c), the binding energy dependent molecular orbital isosurfaces are shown. The calculated spectrum reveals the HOMO, associated with an orbital energy of 4.67 eV, to be a σ state, characteristic of the S–Au interface [cf. Fig. 3(a)] and is formed as a result of direct wave function mixing/hybridization between *p*-like S states and *d*-like states of Au. This state is thought to have been formed upon interaction of localized orbitals with narrow band dispersive electron states.[30] Thiols bind covalently to Au, but with a partially ionic Au–thiolate bond, which is an extra unwanted dipolar layer, or Schottky barrier The Au–thiolate bond has a homolytic bond strength of 40–45 kcal/mol[31] and contributes to stability of SAMs together with the van der Waals forces (1.4–1.8 kcal/mol) between adjacent methylene groups that account for the nearly all-trans configuration. The C–S bond in the thiolates adsorbed on Au(111) are stronger than Ag(111), consistent with the enthalpy of activation[32] $\Delta H_f(Au_2S) = +29$ kJ/mol versus $\Delta H_f(Ag_2S) = -32$ kJ/mol. In most previous articles,[7,33–35] finding the relative position of the Fermi level to HOMO after adsorption of the thiol on Au(111) surface was difficult and conductance in the HOMO–LUMO gap was found to be extremely sensitive to the Fermi level position. However, for alkanes and wide gap molecular solids, the work function changed where the HOMO was tied to vacuum. Rieley *et al.*[36] attributed the observed chemical shifts in near edge x-ray absorption fine structure sulphur *K*-edge spectra of a monolayer of functionalized octanethiol to the presence of surface-bound thiolate (RS^-) and sulphonate (RSO_3^-) species. These authors through UPS measurements showed a clean and low intense S–Au interface band immediately below the Fermi level, which was attenuated with increasing coverage, consistent with the formation of an overlayer on the surface. Molecular dynamics simulation[22] of long chain thiols using *ab initio* geometry optimization of HS and CH_3S on cluster models of Au(111) suggested the existence of two chemisorption modes of thiolates on Au(111), one state had a Au–S–C bond angle of ~180° (*sp* hybridization) and the other has a Au–S–C bond angle of ~104° (*sp*3 hybridization). In a recent paper, Yourdshahyan and Rappe[37] showed the most preferable site for thiolate adsorption on Au(111) is the bridge site with a lower coordination over the higher coordinated fcc site. The structural parameters, such as

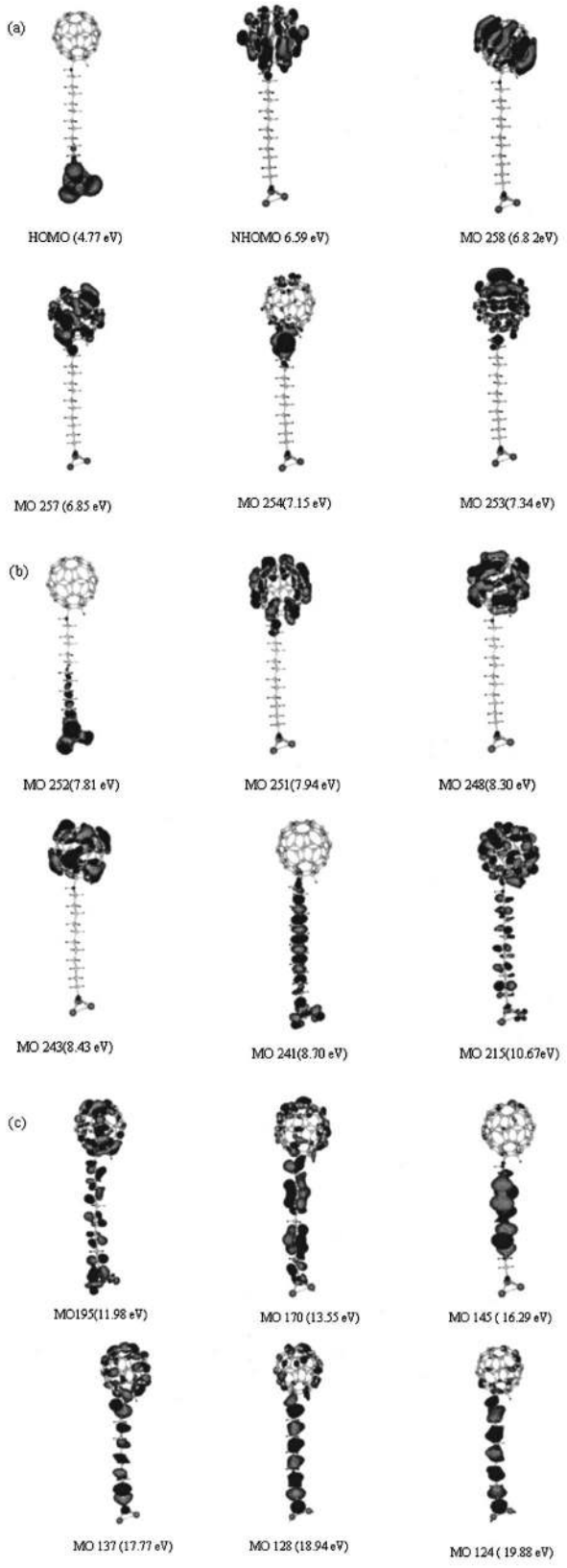

FIG. 3. Typical molecular orbitals from linear combination of atomic orbital approach, covering different energy regions [(a), (b), and (c)] of the UPS of C_{60}-11-AUT SAM. The binding energy was shifted 0.5 eV to fit the experimental spectrum.

d_{S-Au}, and the Au–S–C angle for methyl thiolate showed a preferred Au–S–C angle of ~105°–115°. The existence of such an angular preference, which is similar to the C–C–S bond angle of 108°–116° indicated a distinct directionality for the S–Au bonds at the surface.

D. Bonding states in C_{60}-11-AUT SAM on Au(111)

The near HOMO region of C_{60}-11-AUT SAM in Fig. 2(a) is represented as a deconvoluted first derivative plot in Fig. 2(c). The bonding orbitals well below the HOMO at 3.67 eV contribute to chemisorption of the C_{60} bonded aminothiol on Au(111). The fivefold degeneracy of HOMO of C_{60} is lifted upon the nucleophilic addition of $-NH_2$ group, resulting in a symmetry change from I_h in the former to C1 in the corresponding C_{60}-11-AUT SAM on Au(111). The calculated next HOMO of C_{60}-11-AUT SAM at 6.59 eV in Fig. 3(a) tallies with the 6.6 eV feature in the fitted UPS in Fig. 2(c) showing the $-NH_2$ addition/bonding to C_{60}. The 7.3 and 7.8 eV features in the deconvoluted UPS are represented by molecular orbitals (MOs) 253 and 251 illustrating the respective orbital contributions. The low intensity 8.4 eV UPS band in Fig. 2(c) can be ascribed to the shifted next HOMO of pure C_{60} as shown in Fig. 3(b) at 8.43 eV, in reference to its HOMO at 6.82 eV. The calculated MOs of the SAM thus reveal that upon C–N bond formation through the nucleophilic addition, the position of C_{60} HOMO (MO 258) in Fig. 3(a) at 6.82 eV [not observed experimentally in Fig. 2(c)] remains constant, while the next HOMO (NHOMO) of C_{60} (MO 213) at 8.43 eV in Fig. 3(b), seen with a weak intensity at 8.4 eV in the experimental spectrum in Fig. 2(c), has shifted to higher binding energy by 0.2 eV.

In order to explain further the cause of such low intensity in the UPS and to learn whether the observed low intensity is a collective property of the film, or a property of the C_{60} molecules that comprise the film, we have investigated the photoemission characteristics of a thick, 140 nm C_{60} film evaporated on the Au(111) surface. The results are shown in Fig. 4. In Fig. 4(a), the nearly clean Au UPS features represent Au *d* bands with Fermi edge at 4.7 eV. These bands are buried completely in the spectrum for the C_{60} film. Clear bands of HOMO and NHOMO for the C_{60} film at 6.8 and 8.1 eV with a separation of 1.3 eV match the reported values well.[38] The high symmetry of a free C_{60} molecule leads to the highly degenerate and narrow featured DOS in Fig. 4(b). The HOMO and NHOMO bands are observed separately from the other valence bands. The calculated DOS in Fig. 4(b) is shown with longitudinal bars representing binding energy of each state calculated using the restricted Hartree–Fock (RHF) method with 6-31+G* basis set. The DOS curve implies the π dominant HOMO and NHOMO states, attributed to h_u (fivefold degenerate) and h_g+g_g (ninefold degenerate) orbitals in the I_h point group, respectively. However, the calculated intensities are not compared with the experimental intensities. The features immediately after the NHOMO represent σ and π states of C_{60}. A work function change from pure Au at 4.7 eV to 3.9 eV for the adsorbed C_{60} film on Au is observed in Fig. 4(a). Tzeng *et al.*[39] reported a work function decrease to 4.7 eV for 1 monolayer

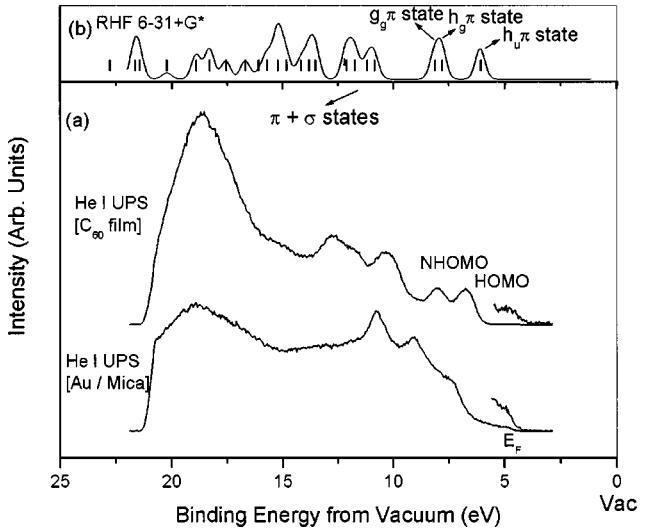

FIG. 4. (a) UPS features of ~140 nm C_{60} film on Au(111) and the corresponding Au(111) bands for Au/mica substrates. (b) Calculated DOS of C_{60} with RHF/6-31+G* method. The longitudinal bars represent energy levels of MOs. The HOMO (h_u) and the NHOMO (h_g+g_g) are the π dominant states. The DOS curve is shifted 1.9 eV towards low binding energy scale to fit the experimental bands.

C_{60}/Au(111) as against a value of 5.3 eV for the pure gold surface. The effect was explained in terms of metallic character of the chemisorbed C_{60} layer as a result of charge transfer from the substrate. Thus from Figs. 2, 3, and 4, we confirm that the valence band photoemission spectra point to the formation of a localized σ(S–Au) bond at the interface and a covalent bond as a result of direct overlap and hybridization between N Pz of the $-NH_2$ group of thiolate SAM and π levels of C_{60}, resulting in a change of symmetry from I_h in C_{60} to C1 in the C_{60}-11-AUT SAM. The low intensity associated with the HOMO and near HOMO spectral features in Fig. 2(a) is a characteristic of the film.

E. The energy level diagram

The above experimental results dictate the interfacial electron energy level diagram as shown in Fig. 5, depicting the HOMO–LUMO gap of C_{60}-11-AUT SAM. The energy alignment in Fig. 5(b) is from the UPS with respect to the Au Fermi level in Fig. 5(a) and without considering possible band bending. The ionization energy, defined as the energy of the HOS relative to vacuum level, is 4.1 eV for the adsorbed C_{60}-11-AUT SAM on Au(111). Figure 5(b) is derived for the energy of the LUMO edge with respect to vacuum level. This could be obtained from the energy of the $\pi-\pi^*$ gap from the shakeup satellite feature in the XPS spectrum. The latter accrues to the fact that conjugated C_{60} has its delocalized electronic π and π^* states and $\pi-\pi^*$ transition could be detected from the shakeup peak on the high binding energy side of the main core level peaks in the XPS spectrum.[40,41] Figure 6 shows the C 1*s* XPS core level features upon Voigt-like function fitting of the experimental data. The peak at 289.1 eV, 4.6 eV from the core C 1*s* feature at 284.5 eV, is attributed to the C 1*s* shakeup satellite feature as a result of π electron transition from the occupied to the unoccupied valence molecular orbitals ($\pi-\pi^*$ transition) as-

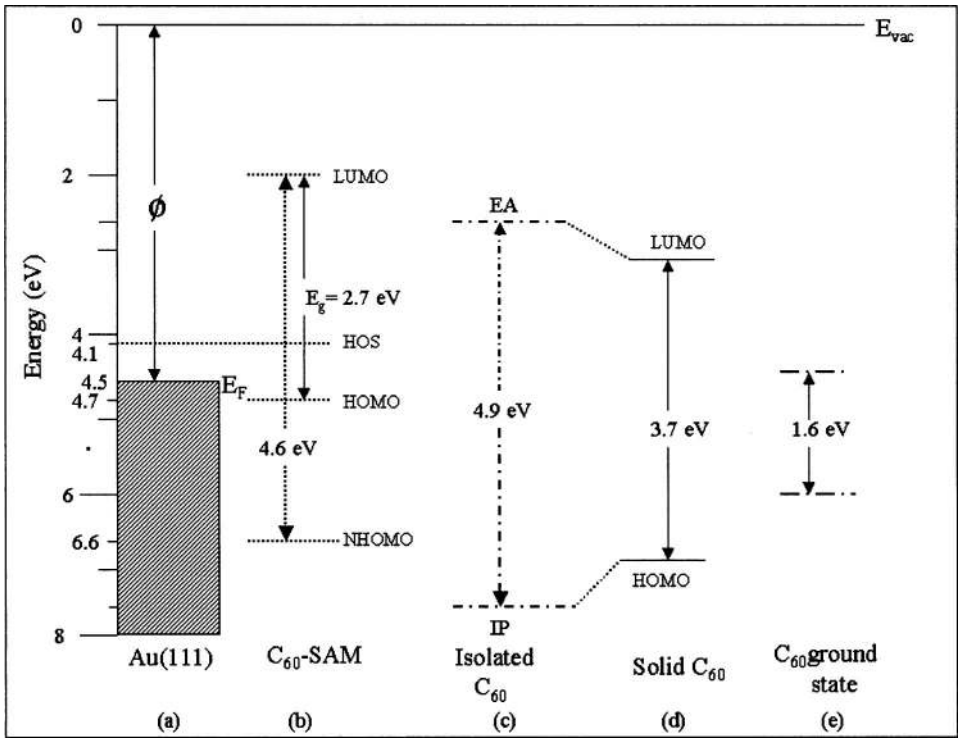

FIG. 5. Diagram for energy level alignment as derived from: (a) UPS, (b) UPS and XPS, and (c), (d), (e) (vide Ref. 42).

sociated with the C 1*s* core hole generation. C 1*s* shakeup features of C_{60} have been studied intensely both theoretically[42] and experimentally with thick films of C_{60}. In the shakeup energy range of 5–10 eV from the main line at 284.5 eV in the high resolution XPS spectrum, four shakeup structures were immediately noticeable at 1.8, 3.7, 4.8, and 5.9 eV. The intensity of the shakeup feature in the present work constitutes ~4% of the main peak. Ohno *et al.*[43] while experimenting with C_{60} multilayers on Au, found the HOMO–LUMO gap to be 3.7 eV with $\pi-\pi^*$ shakeup peaks extending at least 7 eV higher over the main C 1*s* feature at 285 eV.

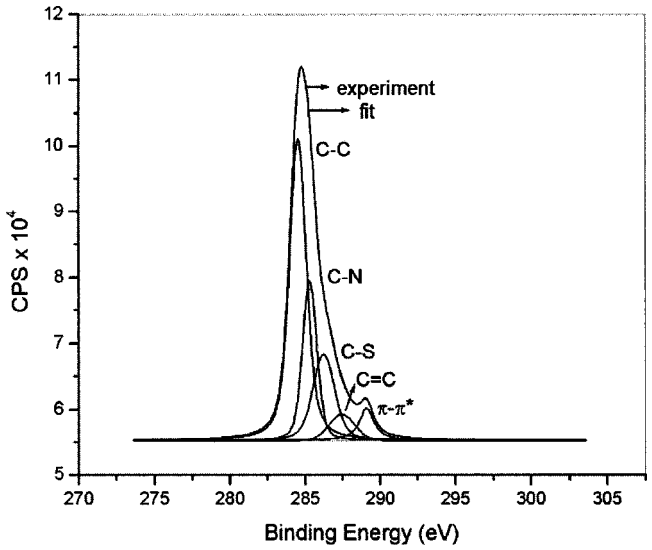

FIG. 6. XPS of C_{60}-11-AUT SAM showing $\pi-\pi^*$ shakeup satellite peak at 289.1 eV.

In Fig. 7, the orbital diagrams for LUMO levels are depicted. It is simpler to understand the nature of conduction peaks from the MO electron density distributions. The nondegenerate LUMO, LUMO+1, and LUMO+2 are entirely localized on the C_{60} cage and correspond to its π feature, while that in pure C_{60} states are degenerate. The LUMO+1

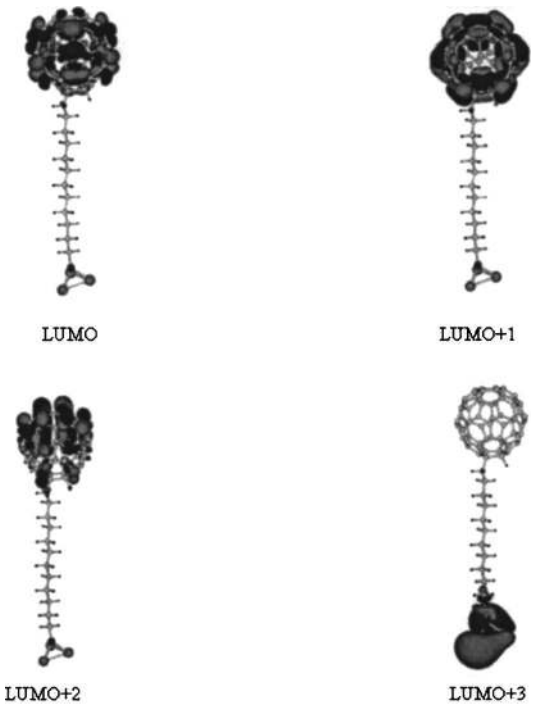

FIG. 7. LUMOs of C_{60}-11-AUT SAM, calculated from DFT with B3LYP correlation.

state is one of the triply degenerate LUMOs of C_{60} having the largest spatial extent due to larger overlap with neighboring molecules.[44] However, the LUMO is more important for conduction from energy considerations. There is no mixing of the above three LUMOs with the sulfur *p* orbitals or with Au *d* orbitals. However, LUMO+3 at a much higher energy seems to be localized at the interface, bearing a different isosurface than the interface σ(S–Au) HOMO.

The π-state level in Fig. 5(b) cannot be aligned with the HOMO of C_{60}-11-AUT SAM since the latter is a σ state, but could be aligned with the next HOMO (NHOMO), which is a π state of the C_{60} anchored SAM, observed at 6.6 eV in Fig. 2(c) with its MO diagram in Fig. 3(a). Hence taking into consideration the 4.6 eV π–π^* gap from XPS results, the LUMO level of the adsorbed SAM on Au(111) lies at 2.0 eV (including the exciton binding energy) in the energy scale as shown in Fig. 5(b). This leads to the assignment of the electronic band gap E_g to be the energy difference between the HOMO and the LUMO levels of C_{60}-11-AUT SAM as 2.7 eV. In the present scenario, the placement of E_F much below the mid gap and closer to HOMO implies the SAM to be a *p*-type semiconductor. Except for LUMO+3, the molecular orbital isosurfaces depicted for LUMO, LUMO+1, and LUMO+2 in Fig. 7 indicate the electron density to be localized over the C_{60} cage, which further validates taking the NHOMO state as the threshold for the π–π^* gap. The LUMO level in the Alq_3 layer on Al,[45] with respect to vacuum, was determined taking into consideration the HOS and an observed optical band gap of 2.8 eV which was 0.3–0.4 eV smaller than E_g. HOMO–LUMO gaps in molecules containing alkyl chains have been reported,[46,47] however, no experimental data exist for the same for Au/alkanethiol SAM. ~8 eV as the common value has been taken for alkanethiol systems.[48] HOMO–LUMO gaps for the SAM of *n*-alkyltrichlorosilane molecules $[CH_3(CH_2)_{n-1}SiCl_3]$ with chain length $n=12$, 16, 18 on naturally oxidized silicon wafers were obtained in the range of 9.2–9.9 eV$\pm$0.3 eV for all C12, C16, and C18 SAMs. For all-trans alkane chains, semiempirical calculations in the tight-binding approximation[49] predicted ~11 and ~12 eV for C18 and C10, respectively, implying a highly insulating character of these SAMs. Wang *et al.*[48] investigated the mechanism of electron transport through SAMs of alkane thiols of varying chain length using a device structure. Temperature independent electron transport was observed in dodecane thiol (C_{12}), providing evidence for direct tunneling as the dominant conduction mechanism with a barrier height of 1.40$\pm$0.02 eV. The latter was based on the fact that the Fermi levels of the contacts lie within the HOMO–LUMO gap.

In Figs. 5(c), 5(d), and 5(e), energy level diagrams according to Ohno *et al.*[43] are shown with respect to vacuum level for isolated C_{60} with its ionization potential and electron affinity levels, for the solid with $N\pm1$ electrons showing the HOMO–LUMO derived bands and for the ground state of C_{60} with *N* electrons, respectively. We emphasize that while in the C_{60}-11-AUT SAM, the HOMO is a σ state from interface atomic orbital mixing between S and Au, the LUMO is a π^* state, accrued from the delocalized π network of C_{60}. Further, the HOMO–LUMO gap in the C_{60}-11-AUT SAM has reduced to 2.7 eV as compared to a large band gap of ~8 eV in alkane thiols. In long molecular wires, the unoccupied level participating in conduction should be a delocalized π^* state which in the conjugated cage network cannot couple with the σ(S–Au) HOMO at the interface because of the spatial separation and symmetry variation between them. This molecule also commensurates with the fact that for a molecular wire conductance, the strength of the bond at the interface should be strong, simultaneously keeping the intramolecular binding intact. In the energy level diagram, underestimating the influence of dipolar potential at the interface, the barrier height for electron injection from the substrate is the energy difference between the Fermi level of Au(111) and the LUMO edge of the SAM, which amounts to 2.5 eV. This barrier height is much lower than the normal alkanethiol SAMs (HOMO–LUMO) gap of ~8 eV on Au(111) and is one of the important factors that can significantly contribute to the lowering of driving voltage in a device made with the above SAM on Au(111) as the cathode. It is worth mentioning here that the UPS spectral features of the C_{60} functionalized SAM at elevated temperatures were hardly affected until 145 °C, implying stability and rigidity associated with the film and the interface S–Au bond. No shift in the Fermi level over the whole temperature range was observed. At 265 °C, although no remarkable effect was seen, partial desorption was imminent in the alkyl chain region as well as in the bonded C_{60} region. The latter seemed irreversible after cooling to room temperature.

IV. CONCLUSION

While the molecular orientation is dependent on the packing density, the ordering of the molecular arrangement, indispensable for self assembly, depends on the balance between the structures demanded by intermolecular and molecule–substrate interactions. We have carried out a systematic study on the electronic structure of the C_{60} functionalized aminothiol self-assembled monolayers on the Au(111) surface using surface sensitive UPS that probes the occupied molecular orbitals. The results revealed drastic modifications to *d*-band structure of Au(111) and the electronic structure was found sensitive towards the S–Au interface and the C_{60} end functional moiety with formation of localized σ(S–Au) and σ(N–C) bonds, respectively. Thermal desorption measurements, performed in order to obtain the strength of the monolayer–metal interaction, revealed the interface to be strong and with negligible desorption of C_{60}. While in the C_{60}-11-AUT SAM, the HOMO is found to be a σ state, the LUMO is a π^* state, accrued from the delocalized π network of C_{60}. The drastically reduced HOMO–LUMO gap of 2.7 eV in the C_{60}-11-AUT SAM, as compared to a large electronic gap of ~8 eV in alkanethiols, enables it to be a potential electron transport medium.

ACKNOWLEDGMENTS

Japan Society for Promotion of Sciences (JSPS) is gratefully acknowledged for granting the invitation fellowship to A.P. A.P. thanks Rashmi R. Sahoo for loaning the gold

plates, Hiroyuki Yamane for XPS spectral acquisition, and Dr. Satoshi Kera for his many sided help towards the experiments.

[1] M. A. Reed, C. Zhou, C. J. Muller, T. P. Burgin, and J. M. Tour, Science **278**, 252 (1997).
[2] J. Chen, M. A. Reed, A. M. Rawlett, and J. M. Tour, Science **286**, 1550 (1999).
[3] M. Magoga and C. Joachim, Phys. Rev. B **57**, 1820 (1998).
[4] S. N. Yaliraki and J. Ratner, J. Chem. Phys. **109**, 5036 (1998).
[5] J. M. Seminario, A. G. Zacarias, and J. M. Tour, J. Am. Chem. Soc. **121**, 411 (1999).
[6] E. G. Emberly and G. Kirczenow, Phys. Rev. B **58**, 10911 (1998).
[7] W. Tian, S. Datta, S. Hong, R. Reifenberger, J. I. Henderson, and C. P. Kubiak, J. Chem. Phys. **109**, 2874 (1998).
[8] T. Vondrak, H. Wang, P. Winget, C. J. Cramer, and X. Y. Zhu, J. Am. Chem. Soc. **122**, 4700 (2000).
[9] T. Vondrak, C. J. Cramer, and X. Y. Zhu, J. Phys. Chem. B **103**, 8915 (1999).
[10] S. Kera, H. Setoyama, K. Kimura, A. Iwasaki, K. K. Okudaira, Y. Harada, and N. Ueno, Surf. Sci. **482–485**, 1192 (2001).
[11] K. Kim, H. Song, J. T. Park, and J. Kwak, Chem. Lett. **2000**, 532.
[12] K. Chen, W. B. Caldwell, and C. A. Mirkin, J. Am. Chem. Soc. **115**, 1193 (1993).
[13] W. B. Caldwell, K. Chen, C. A. Mirkin, and S. J. Babinec, Langmuir **9**, 1945 (1993).
[14] Y. S. Shon, K. F. Kelly, N. J. Hallas, and T. R. Lee, Langmuir **15**, 5329 (1999).
[15] D. Hirayama, K. Takimiya, Y. Aso, T. Otsubo, T. Hasobe, H. Yamada, H. Imahori, S. Fukusumi, and Y. Sakata, J. Am. Chem. Soc. **124**, 532 (2002).
[16] A. E. Hooper, D. Werho, T. Hopson, and O. Palmer, Surf. Interface Anal. **31**, 809 (2001).
[17] F. Diederich, J. Effing, U. Jonas, L. Jullien, T. Plesnivy, H. Ringsdorf, C. Thilgen, and D. Weinstein, Angew. Chem., Int. Ed. Engl. **31**, 1599 (1992).
[18] A. E. Hooper, D. Werho, T. Hopson, and O. Palmer, Surf. Interface Anal. **31**, 809 (2001).
[19] M. J. Frisch *et al.*, GAUSSIAN 98 User's Reference, Gaussian Inc., Pittsburg, PA, 1998.
[20] A. D. Becke, J. Chem. Phys. **98**, 5648 (1993).
[21] C. Lee, W. Yang, and R. G. Parr, Phys. Rev. B **37**, 785 (1988).
[22] P. J. Hay and W. R. Wadt, J. Chem. Phys. **82**, 270 (1985).
[23] H. Sellers, A. Ulman, Y. Shnidman, and J. E. Eilers, J. Am. Chem. Soc. **115**, 9389 (1993).
[24] A. Johansson and S. Strafstroem, Chem. Phys. Lett. **322**, 301 (2000).
[25] G. M. Whitesides and P. E. Laibinis, Langmuir **6**, 87 (1990).
[26] J. M. Seminario, A. G. Zacarias, and J. M. Tour, J. Am. Chem. Soc. **121**, 411 (1999).
[27] D. Yoshimura, H. Ishi, S. Narioka, M. Sei, T. Miyazaki, Y. Ouchi, S. Hasegawa, Y. Harima, K. Yamashita, and K. Seki, J. Electron Spectrosc. Relat. Phenom. **78**, 359 (1996).
[28] K. Kimura, S. K. Katsumata, Y. Achiba, T. Yamazaki, and S. Iwata, *Handbook of HeI Photoelectron Spectra of Fundamental Organic Molecules* (Japan Scientific Societies Press, Tokyo, 1981).
[29] A. Abduaini, S. Kera, M. Aoki, K. K. Okudaira, N. Ueno, and Y. Harada, J. Electron Spectrosc. Relat. Phenom. **88–91**, 849 (1998).
[30] R. Felice, A. DiSelloni, and E. Molinari, J. Phys. Chem. B **107**, 1151 (2003).
[31] G. M. Whitesides and P. E. Laibinis, Langmuir **6**, 87 (1990).
[32] D. M. Jaffery and R. J. Madix, Surf. Sci. **311**, 159 (1994).
[33] V. Mujica, M. Kempp, and M. A. Ratner, J. Am. Chem. Soc. **101**, 6849 (1994).
[34] E. G. Emberly and G. Kirczenow, in *Molecular Electronics: Science and Technology*, edited by A. Aviram and M. A. Ratner, Annals of the New York Academy of Sciences, Vol. 852 (New York Academy of Sciences, New York, 1998), p. 54.
[35] P. Sautet and C. Joachim, Chem. Phys. Lett. **153**, 511 (1988).
[36] H. Rieley, N. J. Price, R. G. White, R. I. R. Blynth, and A. W. Robinson, Surf. Sci. **331–333**, 189 (1995).
[37] Y. Yourdshahyan and A. M. Rappe, J. Chem. Phys. **117**, 825 (2002).
[38] S. Hasegawa, T. Miyamae, K. Yakushi, H. Inokuchi, K. Seki, and N. Ueno, Phys. Rev. B **58**, 4927 (1998).
[39] C. T. Tzeng, W. S. Lo, J. Y. Yuh, R. Y. Chu, and K. D. Tsuei, Phys. Rev. B **61**, 2263 (2000).
[40] B. Sjoegren, W. R. Salaneck, and S. Stafstroem, J. Chem. Phys. **97**, 137 (1992).
[41] W. R. Salaneck, S. Stafstroem, and J. L. Bredas, *Conjugated Polymer Surface and Interfaces* (Cambridge University Press, Cambridge, 1996), p. 39.
[42] C. Enkvist, S. Lunell, B. Sjogren, S. Svensson, P. A. Bruehwiler, A. Nilsson, A. J. Maxwell, and N. Martensson, Phys. Rev. B **48**, 14629 (1993).
[43] T. R. Ohno, Y. Chen, S. E. Harvey, G. H. Kroll, J. H. Weaver, R. E. Haufler, and R. E. Smalley, Phys. Rev. B **44**, 13747 (1991).
[44] P. A. Bruehwiler, P. A. Maxwell, J. Rudolf, C. D. Gutleben, B. Waestberg, and N. Martensson, Phys. Rev. Lett. **71**, 3721 (1993).
[45] K. L. Wang, B. Lai, M. Lu, X. Zhou, L. S. Liao, X. M. Ding, X. Y. Hou, and T. S. Lee, Thin Solid Films **178**, 178 (2000).
[46] C. Boulas, F. Davidovits, F. Rondelez, and D. Vuillaume, Phys. Rev. Lett. **76**, 4797 (1996).
[47] S. G. Lias, J. E. Bartmess, J. F. Liebman, J. L. Holmes, R. D. Levin, and W. G. Mallard, J. Phys. Chem. Suppl. **17**, 1 (1988).
[48] W. Wang, T. Lee, and M. A. Reed, Phys. Rev. B **68**, 035416 (2003).
[49] J. Robertson, Philos. Mag. B **66**, 615 (1992).